Affordable full subsurface image volume—an application to WEMVA

T. van Leeuwen[1], R. Kumar[2] and F. J. Herrmann[2]
[1] Mathematical Institute, Utrecht University, The Netherlands
[2] Seismic Laboratory for Imaging and Modeling (SLIM), University of British Columbia, Canada

Abstract

Common image gathers are used in building velocity models, inverting for anisotropy parameters, and analyzing reservoir attributes. In this paper, we offer a new perspective on image gathers, where we glean information from the image volume via efficient matrix-vector products. The proposed formulation make the computation of full subsurface image volume feasible. We illustrate how this matrix-vector product can be used to construct objective functions for automatic MVA.

Introduction

An extended image is a multi-dimensional correlation of source and receiver wavefields, as a function of *all* subsurface offsets (see Sava and Vasconcelos, 2011, and references therein for a recent overview). There are many different applications in which extended images are used extensively. A prime example is wave-equation based migration velocity analysis (Biondi and Symes, 2004; Shen and Symes, 2008; Symes, 2008b; Sava and Vasconcelos, 2011), which is based upon the principle that the energy in the common-image gathers (CIG) is focused at zero offset for the correct velocity model. In general, these CIG's (or extended images) are a function of all subsurface-offset and time-lags (or equivalently, frequencies) for all subsurface points using the full two-way wave equation, which is computationally infeasible to compute and store. In this paper, we propose a new way to compute the subsurface image volume without computing the whole source and receiver wavefields. In order to do so, we first write the multi-dimensional correlation as an outer product of the source and receiver wavefields. Then, we probe the full subsurface image volume for information by *matrix-free* multiplication with a vector. We show that such matrix-vector product can be computed cheaply and used to formulate a cost efficient automatic MVA algorithm. Finally, we show the efficacy of the proposed formulation on two different velocity models i.e. horizontal reflectors model embedded with Gaussian anomaly (Lens model) and the Marmousi model.

Affordable image-gathers with WEMVA

Given monochromatic source and receiver wavefields as data matrices U and V, where each column represents the wavefield for a single source, the extended image is given by

$$E = VU^* = H^{-*}P_r^T DQ^* P_s H^{-*}, \qquad (1)$$

where the wavefields U and V are the solutions of a time-harmonic wave equation

$$HU = P_s^T Q, \quad \text{and} \quad H^*V = P_r^T D.$$

Here * denotes the conjugate-transpose, H is a discretization of the Helmholtz operator $(\omega^2 m + \nabla^2)$, m is the squared slowness, the matrix Q represents the sources, D is the data matrix and the matrices P_s, P_r sample the wavefield at the source and receiver positions (and hence, their transpose injects the sources and receivers into the grid). An element e_{ij} of resulting matrix E captures the interaction between gridpoints i and j. All conventional extended images can be extracted from this matrix, for example by selecting only elements with lateral interaction. In order to perform the automatic MVA, Shen and Symes (2008) consider penalizing the extended images as a function of subsurface offset with the lateral shift, which in our case is equivalent to demanding that our image matrix commutes with point-wise multiplication with the $\mathbf{x}$-position. For a focused image, we want to enforce that

$$E\mathrm{diag}(\mathbf{x}) \approx \mathrm{diag}(\mathbf{x})E.$$

The obvious way to achieve this is by formulating the optimization problem as

$$\min_{\mathbf{m}} \phi(\mathbf{m}) = ||E(\mathbf{m})\mathrm{diag}(\mathbf{x}) - \mathrm{diag}(\mathbf{x})E(\mathbf{m})||^2,$$

where $\|.\|$ is a matrix norm. Since H^{-*} in equation (1) represents an adjoint wave-equation solve, which constitutes the main computational cost in forming the extended image. Therefore, it is not feasible to form and compute the proposed objective function using full subsurface image volume. However, If we choose the Frobenius norm as the matrix norm, then we can mitigate this impediment and estimate the proposed objective function efficiently via randomized trace estimation without explicitly forming the whole matrix (Avron and Toledo, 2011). The basic idea is as follows. First, write the Frobenius norm as the matrix trace. Then, the trace can be estimated as

$$||A||_F^2 = \mathrm{trace}(A^TA) \approx \sum_{i=1}^{K} \mathbf{w}_i^T A^T A \mathbf{w}_i = \sum_{i=1}^{K} ||A\mathbf{w}_i||_2^2$$

,

where $\sum_{i=1}^{K} \mathbf{w}_i \mathbf{w}_i^T \approx I$. Thus, the optimization can be written as

$$\min_{\mathbf{m}} \widetilde{\phi}(\mathbf{m}) = \sum_{i=1}^{K} ||R(\mathbf{m})\mathbf{w}_i||^2,$$

where $R(\mathbf{m}) = E(\mathbf{m})\mathrm{diag}(\mathbf{x}) - \mathrm{diag}(\mathbf{x})E(\mathbf{m})$.

Results

We first demonstrate the advantage of randomized trace estimation using a subset of the Marmousi model. Figure 1 shows the true and approximate penalties (in the Frobenius norm) as a function of velocity perturbation for reflected waves. We can clearly see that we only need a few probing vectors to approximate the true objective function. Then, we highlight the computational complexity of the conventional method (Sava and Vasconcelos, 2011) versus the proposed method in terms of the number of sources N_s, receivers N_r sample points N_x and desired number of subsurface offsets (h) in each direction $N_{h_{x,y,z}}$ (Table 1). To illustrate the benefits of the proposed scheme, we also report the computational time (in sec) and memory (in mb) required to compute a single CIP gather for a 2D synthetic (1-layer) model of 51×101 gridpoints, using 25 frequencies and 51 sources and receivers. The results are shown in Table 2. We can see that the on a small toy model, the probing technique reduces the computational time and memory requirements by a factor of 10 and 30, respectively.

Finally, we perform the automatic velocity analysis on two different velocity models. The first example is horizontal reflectors model embedded with Gaussian anomaly (Lens model). To regularize the inversion and impose the smoothness on the gradient, we parameterize the model using cubic B-splines (Symes, 2008a). We perform 30 L-BFGS (Nocedal and Wright, 2000) iterations and choose $K = 100$ in this case. The sampling interval of the B-splines is 36 m. Figures 2 a,d show the corresponding true velocity model and the image gather. The initial model (Figure 2 b) used for WEMVA is a vertical gradient model. The corresponding image gather (Figure 2 e) is defocused. Note that in practice, probably a more accurate starting model can be used, so this can be considered a worst case scenario. Figures 2 c,f show the estimated velocity model and the corresponding image gather. The focused image gathers indicate that we get a good reconstruction of the Gaussian anomaly which is not present in the starting model. The second example is a subset of the Marmousi model as shown in figure 3 (a). We choose $K = 200$ and the sampling interval of the B-splines is 48 m. The initial velocity model, shown in Figure 3 (b), is a highly smoothed version of the true model. Figure 3 (c) shows the inverted model using the proposed formulation after 4 iterations of L-BFGS. The image gathers using the true, initial and inverted models, respectively are shown in figures 3 (d-f). We can see that events are well-focused and at the correct position up to the depth of 1.2 km. We do not expect good results beyond this depth due to limited aperture.

	# of PDE solves	flops
conventional	$2N_s$	$N_s N_{h_x} N_{h_y} N_{h_z}$
this work	$2N_x$	$N_r N_s$

Table 1: Computational complexity of the conventional method versus proposed method in terms of the number of sources N_s, receivers N_r, sample points N_x and desired number of subsurface offsets in each direction $N_{h_{\{x,y,z\}}}$.

Conclusions

We have discussed an efficient way of gleaning information from the full subsurface extended image volume, where we first organize this gigantic extended image volume as a matrix. Then, we compute the action of this matrix on a given vector, without explicitly constructing the whole image volume. We show that how to use such matrix-vector products to formulate a cost efficient function for automatic MVA. The dominant computational cost of each matrix-vector product is 2 PDE solves and does not depend on

	time (s)	memory (mb)
conventional	23.6	103
this work	2.02	0.03

Table 2: Comparison of the computational time (in sec) and storage memory (in megabytes) for computing CIP's gather on a very small model of size 51×101. We can see the significant difference in time and memory usage of the method proposed in this paper compared to the conventional method, even for a small test problem, and we expect this difference to be greatly exacerbated for realistically sized models.

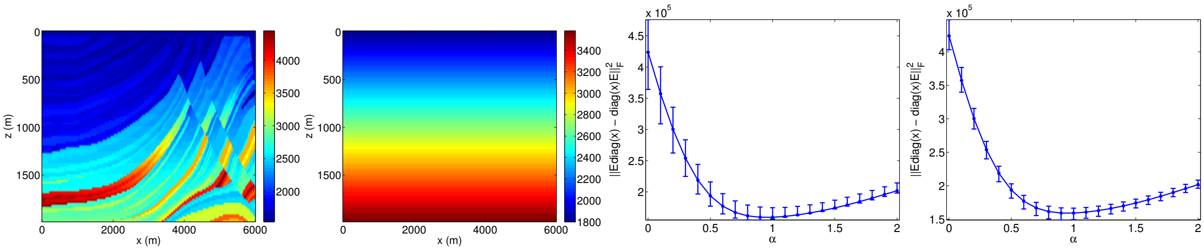

(a) (b) (c) (d)

Figure 1: Randomized trace estimation. (a,b) True and initial velocity model. Objective functions for WEMVA based on the Frobenius norm, as a function of velocity perturbation using the complete matrix (blue line) and error bars of approximated objective function evaluated via 5 different random probing with (c) K=10 and (d) K = 80 for the Marmousi model.

the desired sampling of the subsurface offsets nor the number of sources and receivers, which in turn reduces the significant computational cost of proposed WEMVA objective function.

Acknowledgements

This work was financially supported in part by the Natural Sciences and Engineering Research Council of Canada Discovery Grant (RGPIN 261641-06) and the Collaborative Research and Development Grant DNOISE II (CDRP J 375142-08). This research was carried out as part of the SINBAD II project with support from the following organizations: BG Group, BGP, Chevron, ConocoPhillips, CGG, ION GXT,

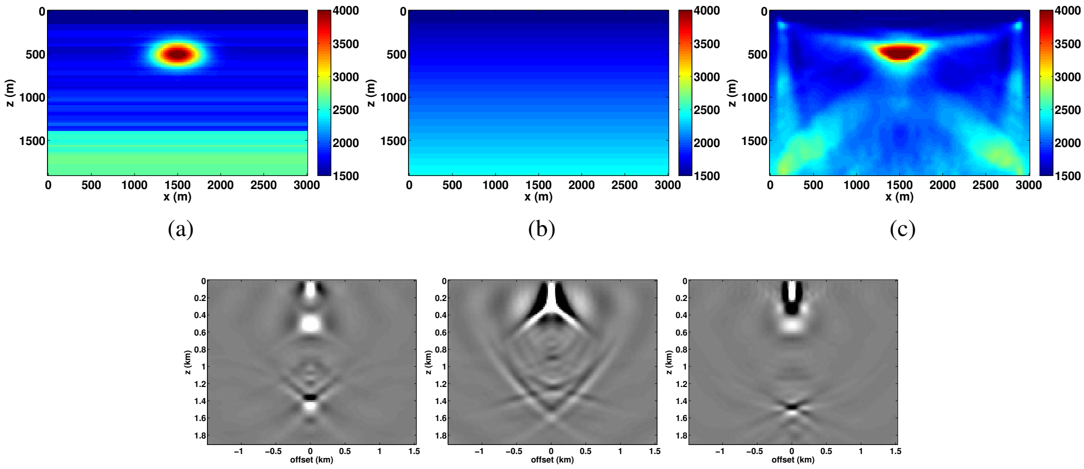

(a) (b) (c)

(d) (e) (f)

Figure 2: Lens model. (a,b,c) True model, initial model and inversion results after 30 iterations. (d,e,f) CIG along $x = 1500$ m and z for true model, initial model and inversion results..

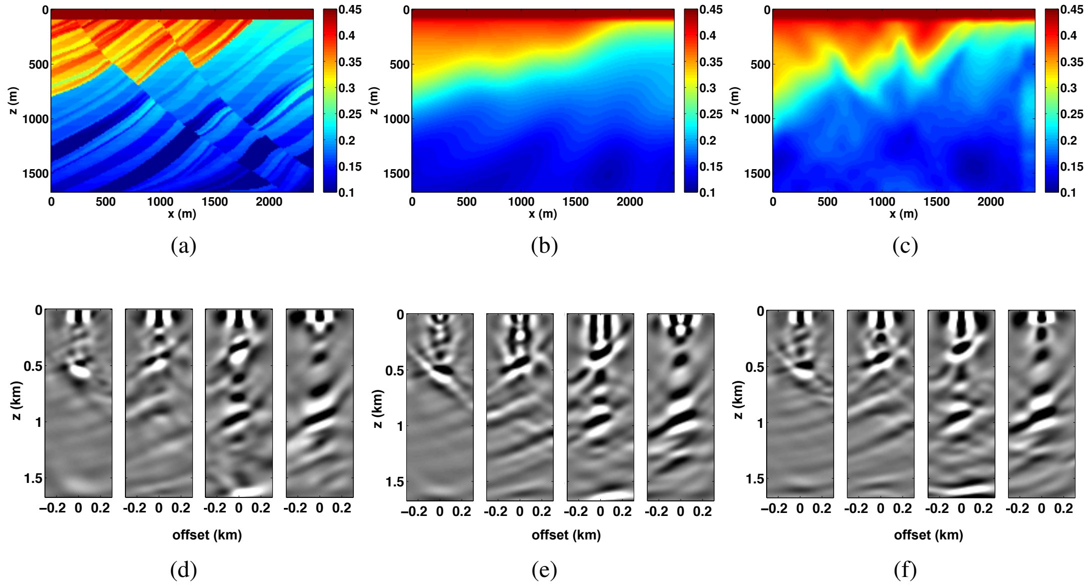

Figure 3: Marmousi model. (Left) True, Initial and Inverted model. (Right) CIG extracted along $x = 680$ m, 1160 m, 1640 m and 2220 m. (Top) True model. (Middle) starting model. (Bottom) Inverted results.

Petrobras, PGS, Statoil, Sub Salt Solutions, Total SA, WesternGeco, Woodside.

References

Avron, H. and Toledo, S. [2011] Randomized algorithms for estimating the trace of an implicit symmetric positive semi-definite matrix. *Journal of the ACM*, **58**(2), 1–16, ISSN 00045411, doi:10.1145/1944345.1944349.

Biondi, B. and Symes, W.W. [2004] Angle-domain common-image gathers for migration velocity analysis by wavefield-continuation imaging. *Geophysics*, **69**(5), 1283.

Nocedal, J. and Wright, S.J. [2000] *Numerical Optimization*. Springer, ISBN 0387987932.

Sava, P. and Vasconcelos, I. [2011] Extended imaging conditions for wave-equation migration. *Geophysical Prospecting*, **59**(1), 35–55, ISSN 00168025, doi:10.1111/j.1365-2478.2010.00888.x.

Shen, P. and Symes, W.W. [2008] Automatic velocity analysis via shot profile migration. *Geophysics*, **73**(5), VE49–VE59.

Symes, W. [2008a] Approximate linearized inversion by optimal scaling of prestack depth migration. *GEOPHYSICS*, **73**(2), R23–R35, doi:10.1190/1.2836323.

Symes, W.W. [2008b] Migration velocity analysis and waveform inversion. *Geophysical Prospecting*, **56**(6), 765–790.